processes

MDPI

Article

Synthesis of γ-AlOOH Nanosheets and Their Adsorption Properties for Heavy Metal Ions

Shile Wang [1], Lili Wang [2], Ruichao Peng [1,*] and Hongding Tang [1,*]

[1] College of Chemistry & Molecular Sciences, Wuhan University, Wuhan 430072, China; shile_wang@whu.edu.cn
[2] CSSC Huangpu Wenchong Shipbuilding Corporation Co., Ltd., Guangzhou 510000, China
* Correspondence: prc@whu.edu.cn (R.P.); chhdtang@whu.edu.cn (H.T.)

Abstract: The lamellar γ-AlOOH nanosheets were rapidly synthesized by high temperature liquid salt as a reaction medium. The micromorphology, crystal structure, and surface valence characteristics of the samples were characterized by XRD, SEM, TEM, BET, and XPS. The results show that the γ-AlOOH nanosheets have a typical layered structure and a large specific surface area. Taking Cu^{2+} as the target heavy metal ion pollutant, the adsorption properties of γ-AlOOH nanosheets have been studied. The results show that γ-AlOOH nanosheets have excellent adsorption properties of Cu^{2+} at pH = 5, and the adsorption capacity is up to 141.1 mg/g, which has potential of applications as heavy metal ion adsorbent for industrial wastewater.

Keywords: γ-AlOOH nanosheets; heavy metal ions; adsorption

1. Introduction

Industrial wastewater that is rich in heavy metal ions (e.g., Cu^{2+}, Pb^{2+}, As^{5+}) is a major source of water pollution. These ions threaten human health through bioaccumulation in the food chain. Given the critical link between water quality and ecological health, the control and remediation of water pollution have garnered widespread attention. Currently, the removal of heavy metal ions from wastewater is a key strategy in water treatment, with common methods including chemical precipitation, biological treatment, and physical adsorption [1–5]. Among them, the chemical precipitation method is mainly through ferrous sulfate or polyferric sulfate as coagulant for coagulation, or through alkali agent for neutralization coagulation and through redox reaction to achieve. The limitation of this process is that the use of chemical agents increases treatment cost, hindering large-scale applications. The biological treatment leverages the structural properties of organisms to remove heavy metal ions. Although bio-adsorbents exhibit strong adsorption capacities, their long processing period and high costs restrict practical use in wastewater treatment. In contrast, physical adsorption is widely employed due to its simplicity, diverse adsorbent options, high adsorption capacity, and reusability. By selecting employed adsorbents, this method enables either universal or selective adsorption of heavy metal ions, thus meeting diverse practical demands [6–8].

Commonly used adsorbents include carbon-based adsorbents (e.g., activated carbon, charcoal, porous carbon) [9–11], metal oxide adsorbents [12–15], and hydroxide adsorbents such as layered double hydroxides (LDHs) [16–18]. Among these, carbon-based adsorbents are widely used due to their low cost; however, their adsorption capacity is limited by specific surface area, and their recovery from aqueous systems remains challenging. Metal oxide adsorbents, such as manganese oxide and iron oxide, often introduce secondary

check for updates

Academic Editor: Enrico Marsili

Received: 9 March 2025
Revised: 24 March 2025
Accepted: 27 March 2025
Published: 31 March 2025

Citation: Wang, S.; Wang, L.; Peng, R.; Tang, H. Synthesis of γ-AlOOH Nanosheets and Their Adsorption Properties for Heavy Metal Ions. *Processes* **2025**, *13*, 1037. https://doi.org/10.3390/pr13041037

Copyright: © 2025 by the authors. Licensee MDPI, Basel, Switzerland. This article is an open access article distributed under the terms and conditions of the Creative Commons Attribution (CC BY) license (https://creativecommons.org/licenses/by/4.0/).

pollution by leaching residual Mn^{2+} or Fe^{3+} ions during adsorption. In addition, the current adsorption materials still have the problem of poor selectivity and regeneration ability, which seriously limits its practical application. Hydroxide adsorbents like aluminum oxyhydroxide (AlOOH) not only exhibit physical adsorption properties but also enable chemical adsorption via surface -OH functional groups, which endow high adsorption capacity. Additionally, AlOOH possesses a layered crystal structure with an interlayer spacing of 6.1 Å, providing abundant active sites, making it a promising candidate for large-scale heavy metal ion removal [19–22]. Nevertheless, the synthesis process for AlOOH hinders its industrial-scale application due to the long synthesis time, such as Yuwen Qi et al. utilized Al-Li alloy chemical milling waste solution (AlCM) to prepare γ-AlOOH as highly efficient adsorbent for Cr(VI). The NaAlO2 in AlCM reacted with H_2O_2 at room temperature for 0.25 h to prepare porous γ-AlOOH bundles [19]. In addition, Yongxing Zhang et al. synthesized the flower-like hierarchical structure of γ-AlOOH by hydrothermal method under 140 °C for 10 h [21].

In this study, γ-AlOOH was synthesized by high temperature liquid salt as a reaction medium. Thanks to the high temperature liquid phase environment, high purity AlOOH nanosheets can be quickly synthesized in about one minute. The salt can be recovered in a simple way. The micromorphology, crystal structure, and surface valence states were systematically characterized. The adsorption characteristics of γ-AlOOH were investigated with Cu^{2+} as the target contaminated ion, and the underlying adsorption mechanisms were elucidated.

2. Experiment

Aluminum sulfate ($Al_2(SO_4)_3 \cdot 18H_2O$, analytical pure, Sinopharm Chemical Reagent Co., Ltd., Shanghai, China), sodium nitrate ($NaNO_3$, analytical pure, Sinopharm Chemical Reagent Co., Ltd., Shanghai, China), copper nitrate ($Cu(NO_3)_2 \cdot 3H_2O$, analytical pure, Sinopharm Chemical Reagent Co., Ltd., Shanghai, China).

2.1. Physical and Chemical Characterization

Field emission scanning electron microscopy (SEM, Zeiss SIGMA, Carl Zeiss AG, Germany), transmission electron microscopy (TEM, JEM-2100, JEOL Ltd., Japan), X-ray diffraction (XRD, XPert Pro, Malvern Panalytical B.V., The Netherlands), automated surface area and porosity analyzer (BET, ASAP 2020, Micromeritics Instrument (Shanghai) Co., Ltd., China), X-ray photoelectron spectroscopy (XPS, ESCALAB 250Xi, Thermo Fisher Scientific Inc., USA), and continuous-source atomic absorption spectrometry (AAS, contrAA700, Analytik Jena AG, Germany).

2.2. Synthesis of AlOOH Nanosheets

A total of 3 g of $NaNO_3$ was weighed into a crucible and heated in a muffle furnace at 350 °C until a transparent liquid salt was obtained. Subsequently, 0.3 g of $Al_2(SO_4)_3 \cdot 18H_2O$ was rapidly added into the liquid salt. After reacting for 1 min, the crucible was quickly removed and allowed to cool to room temperature naturally. Deionized water was then added to the crucible, followed by sonication to dissolve the salt mixture, and vacuum filtration was performed. The product was washed repeatedly with deionized water until the complete removal of residual $NaNO_3$ was achieved and finally dried at 60 °C for 12 h in an oven to yield AlOOH nanosheets. Then, the salt recovered by drying at 60 °C for 12 h and was reused as liquid salt. In order to investigate the effect of reaction time on the morphology of the product, the reaction time was extended to 5 min.

2.3. Cu^{2+} Adsorption Experiments

For the adsorption tests, 0.10 g of γ-AlOOH was weighed into a 100 mL beaker, followed by the addition of 50 mL of the Cu^{2+} solution ($Cu(NO_3)_2 \cdot 3H_2O$ was dissolved in deionized water to obtain a solution with a concentration of 150 mg/L). The pH was adjusted to 2–7 by HNO_3 solution, and the mixture was stirred continuously during the adsorption process under 150 r/min with a temperature of about 25 °C. The concentration of Cu^{2+} ions at varying adsorption times and pH values was determined using atomic absorption spectroscopy (AAS), and the adsorption capacity and removal rate were calculated. Additionally, 0.10 g of γ-AlOOH adsorbent was added to 50 mL of Cu^{2+} solutions with initial concentrations ranging from 50 to 500 mg/L, and the adsorption behavior was investigated at pH 5. To determine the selected adsorption behavior of γ-AlOOH, $MgCl_2$ and NaCl solution with the same molar concentration as Cu^{2+} was used. To evaluate the regeneration properties of the γ-AlOOH, the Cu^{2+}-loaded γ-AlOOH was subjected to regeneration by introducing the 0.1% HNO_3 solution as regenerant.

3. Results and Discussion

The crystal structure of the sample was characterized by X-ray diffraction (XRD). Figure 1a shows the XRD pattern of the synthesized AlOOH. The characteristic peaks at 14.48°, 28.18°, 44.71°, 49.21°, 55.22°, and 71.91° correspond to the (020), (120), (131), (200), (151), and (251) crystal planes of γ-AlOOH (PDF#21-1307), respectively. No impurity peaks were observed, indicating the successful synthesis of pure-phase γ-AlOOH via the high-temperature liquid salt method. The low crystallinity of γ-AlOOH, attributed to the extremely short reaction time, suggests the presence of abundant crystalline defects. These defects likely provide additional adsorption active sites. Furthermore, the schematic illustration of the γ-AlOOH crystal structure (Figure 1b) reveals a layered configuration with an interlayer spacing of 6.1 Å, where [AlO6] octahedra are arranged and interconnected via surface -OH groups.

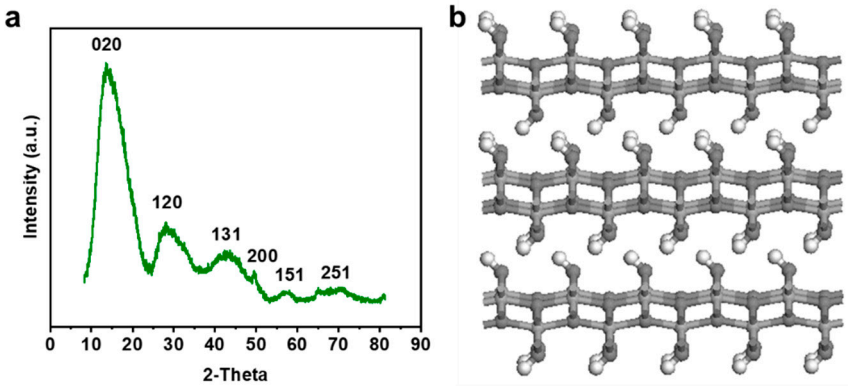

Figure 1. (**a**) XRD pattern of γ-AlOOH; (**b**) schematic diagram of the crystal structure of γ-AlOOH.

The microstructure and morphology of the synthesized γ-AlOOH were characterized by scanning electron microscopy (SEM) and transmission electron microscopy (TEM). As shown in Figure 2a,b, the γ-AlOOH exhibits an ultrathin two-dimensional (2D) nanosheet morphology. The presence of multidirectional wrinkles effectively mitigates stacking-induced agglomeration of the nanosheets, thereby facilitating the exposure of adsorption active sites. Furthermore, high-resolution TEM (HRTEM) and selected-area electron diffraction (SAED) patterns (Figure 2c) reveal the low crystallinity and polycrystalline nature of γ-AlOOH, which is consistent with the XRD results. However, the morphology of γ-AlOOH will change from nanosheets to chaotic nanowires as the reaction time is extended to 5 min (Figure 2d).

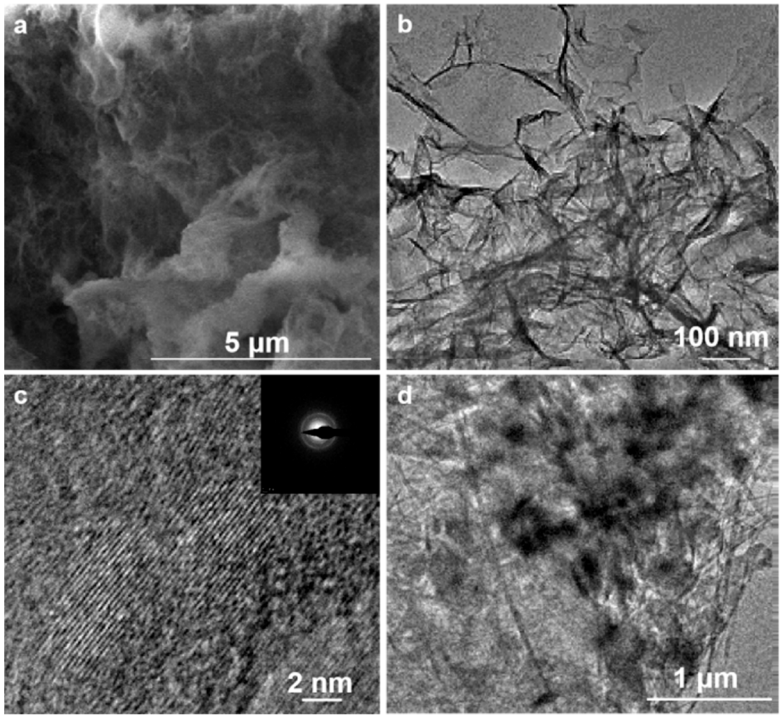

Figure 2. (**a**) SEM pattern of γ-AlOOH with reaction time of 1 min; (**b**) TEM pattern of γ-AlOOH; (**c**) high-resolution TEM pattern and selected area electron diffraction pattern of γ-AlOOH; (**d**) SEM pattern of γ-AlOOH with reaction time of 5 min.

The adsorption capacity of physical adsorption is generally proportional to the specific surface area of the adsorbent. The N_2 adsorption–desorption isotherm of the synthesized γ-AlOOH nanosheets was measured to characterize their specific surface area and pore structure. As shown in Figure 3, the isotherm exhibits an H3-type hysteresis loop without a distinct saturation plateau, indicating a heterogeneous pore structure. The calculated specific surface area of the γ-AlOOH nanosheets is 178.6 m^2/g and with an average pore diameter of 10.4 nm, demonstrating their potential for heavy metal ion adsorption. The high specific surface area not only increases the density of the active site but also promotes the contact probability between ions in the solution and the surface of the adsorbent, thereby increasing the adsorption capacity. In addition, the nanopore network can shorten the ion diffusion path and accelerate the adsorption kinetics.

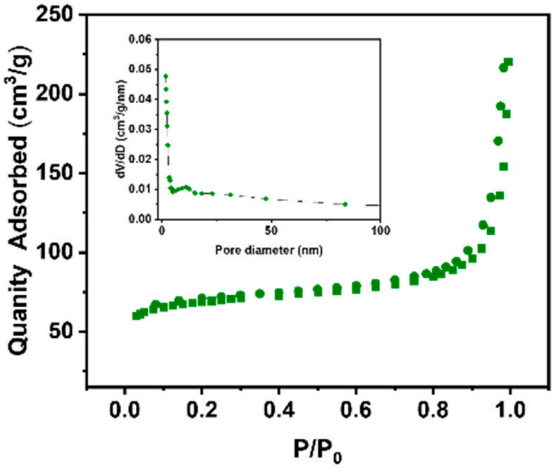

Figure 3. N_2 adsorption and desorption isotherm of γ-AlOOH.

The surface valence states of γ-AlOOH nanosheets significantly influence their adsorption performance. As revealed by the Al 2p (Figure 4a) and O 1s (Figure 4b) XPS spectra, aluminum in γ-AlOOH exists predominantly in the +3 oxidation state, while oxygen is present in two distinct forms: Al–O–Al and Al–O–H. This confirms the abundance of surface -OH groups on the γ-AlOOH nanosheets. Hydroxyl groups are polar groups with lone-pair electron and proton activity and can interact with heavy metal ions in the following ways: (1) Coordination ability: Oxygen atoms provide lone pairs of electrons that form coordination bonds with heavy metal ions; (2) Surface charge regulation: The protonation/deprotonation state of the hydroxyl group affects the surface charge of the adsorbent, which in turn regulates the electrostatic adsorption capacity.

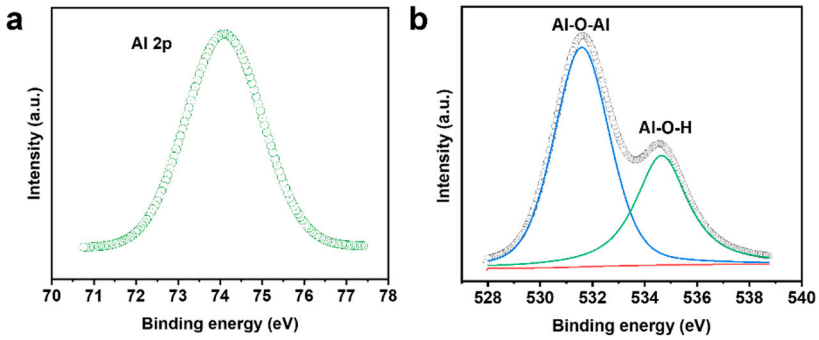

Figure 4. XPS pattern of γ-AlOOH (**a**) Al 2p; (**b**) O 1s.

The above characterizations demonstrate that the layered γ-AlOOH nanosheets synthesized via the high-temperature liquid salt exhibit a high specific surface area and abundant surface functionalities. Compared to conventional liquid-phase synthesis methods (e.g., hydrothermal or sol–gel approaches), the high-temperature liquid salt provides elevated reaction temperatures, which accelerate ion transport. Consequently, ultrathin γ-AlOOH nanosheets with a two-dimensional (2D) lamellar morphology can be synthesized rapidly without requiring surfactants or soft templates, offering economic advantages. Leveraging the structural and morphological features of γ-AlOOH nanosheets, their application as adsorbents for heavy metal ions was explored. For adsorption experiments, 0.1 g of γ-AlOOH nanosheets was added to 50 mL of Cu^{2+} solutions with concentrations ranging from 50 to 500 mg/L. The mixtures were continuously stirred at room temperature for 10 min to 5 h, with pH adjusted to 2–7. The Cu^{2+} removal efficiency was measured using AAS, and the adsorption capacity was calculated accordingly.

Figure 5a illustrates the pH-dependent adsorption behavior of γ-AlOOH nanosheets. The Cu^{2+} removal efficiency increased with rising pH, reaching 17.3% at pH 2 and plateauing at 99.7% at pH 5. At low pH values, the adsorption capacity was suppressed due to competitive adsorption between H^{+} and Cu^{2+} ions. Figure 5b shows the time-dependent adsorption performance at pH 5. The Cu^{2+} removal efficiency rose from 34.9% at 10 min to 99.5% at 1 h, indicating rapid adsorption equilibrium within 1 h. The influence of initial Cu^{2+} concentration is presented in Figure 5c,d. As shown in Figure 5c, the removal efficiency decreased with increasing initial concentration, achieving 56.4% after 2 h at 500 mg/L. The calculated adsorption capacity (Figure 5d) reached a maximum of 139.05 mg/g at 300 mg/L and plateaued at 141 mg/g at 500 mg/L, suggesting saturation of active sites beyond this concentration. This adsorption capacity is considerably competitive with other adsorbents, as shown in Table 1. The superior adsorption performance of γ-AlOOH nanosheets can be attributed to: (1) High surface area and porous structure: The 2D morphology shortens the diffusion path for metal ions and provides abundant physical adsorption sites. (2) Surface functional groups and defects: Surface -OH groups

and crystalline defects act as coordination ligands, enabling chemisorption via chemical complexation. (3) Layered crystal structure: The interlayer spacing (6.1 Å) further enhances adsorption capacity by offering additional active sites.

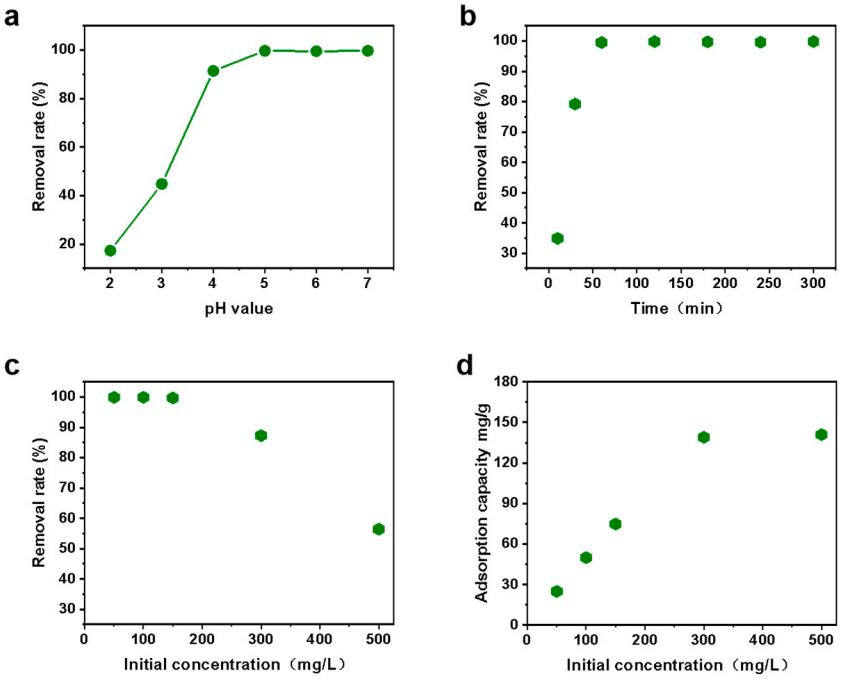

Figure 5. (**a**) The removal rate of Cu^{2+} adsorbed by γ-AlOOH under different pH; (**b**) the removal rate of Cu^{2+} adsorbed by γ-AlOOH under different adsorption time; (**c**) the removal rate of Cu^{2+} adsorbed by γ-AlOOH under different initial concentrations; (**d**) the amount of Cu^{2+} adsorbed by γ-AlOOH at different initial concentrations.

Table 1. Adsorption capacity of different adsorbents for Cu^{2+}.

Sample	Adsorption Capacity	Ref.
Modified Biochar	48.36 mg/g	[23]
Chitosan-coated argillaceous limestone	64.11 mg/g	[24]
Zeolite	124.3 mg/g	[25]
Graphene oxide membranes	72.6 mg/g	[26]
γ-AlOOH nanosheets	**141.1 mg/g**	**This work**

Generally, Mg^{2+} and Na+ existed in wastewater, which will cause a sorption competition toward Cu^{2+} as they all possess the same positive charge. Considering this situation, the adsorption experiments of γ-AlOOH nanosheets on mixed solution of Cu^{2+} and Mg^{2+} or Na^{+} with different molar ratio were tested. In Figure 6a,b, there is only a slit drop in the removal rate of Cu^{2+} as the content of Mg^{2+} or Na^{+} increased in the mixed solution, which indicates the selective adsorption of Cu^{2+} on γ-AlOOH nanosheets again. To satisfy the demand of practical application, five consecutive sorption-desorption cycles were performed. As shown in Figure 6c, the removal rate of γ-AlOOH nanosheets remain as high as 93.3% for Cu^{2+} after five cycles and shows excellent reusability.

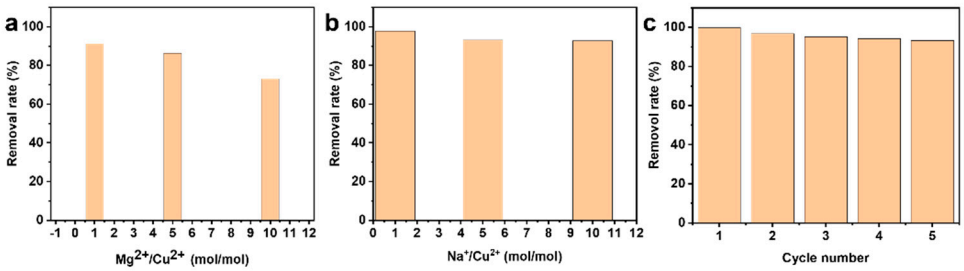

Figure 6. (**a**) Removal rate of Cu^{2+} with γ-AlOOH nanosheets as an adsorbent under different molar ratios of Mg^{2+}/Cu^{2+} in the mixed solution. (**b**) Removal rate of Cu^{2+} with γ-AlOOH nanosheets as an adsorbent under different molar ratios of Na^{+}/Cu^{2+} in the mixed solution. (**c**) Variation in the capacity of Cu^{2+} sorption onto γ-AlOOH nanosheets in successive cycles.

4. Conclusions

The high-temperature liquid salt method enables the efficient and cost-effective synthesis of γ-AlOOH nanosheets. The wrinkled 2D morphology of the nanosheets mitigates layer stacking, resulting in a high specific surface area (178.6 m^2/g), which facilitates enhanced adsorption of metal ions. The adsorption of Cu^{2+} by γ-AlOOH nanosheets involves both physical adsorption and chemisorption. Under optimized conditions (pH 5, room temperature), adsorption equilibrium is achieved within 1 h, with a maximum adsorption capacity of 141 mg/g. At the same time, the liquid salt can be simply recycled and reused, which reduces the production cost and is conducive to the subsequent large-scale production. These findings demonstrate the practical potential of γ-AlOOH nanosheets for treating heavy metal-laden industrial wastewater. The adsorption behavior of γ-AlOOH nanosheets to other heavy metal ions can be further discussed. In addition, it is also important to note that in the reaction environment of high temperature liquid salts, and it is difficult to accurately control the very short reaction time, so it is not easy to obtain uniform morphology of γ-AlOOH nanosheets.

Author Contributions: Methodology, L.W.; Writing—original draft, S.W.; Writing—review & editing, R.P. and H.T. All authors have read and agreed to the published version of the manuscript.

Funding: This research was funded by the National Key Research and Development Program of China (No. 2021YFB2401400).

Data Availability Statement: The original contributions presented in the study are included in the article, further inquiries can be directed to the corresponding authors.

Conflicts of Interest: Author Lili Wang was employed by the company CSSC Huangpu Wenchong Shipbuilding Corporation Co., Ltd. The remaining authors declare that the research was conducted in the absence of any commercial or financial relationships that could be construed as a potential conflict of interest. The company had no role in the design of the study; in the collection, analyses, or interpretation of data; in the writing of the manuscript, or in the decision to publish the results.

References

1. Qasem, N.A.A.; Mohammed, R.H.; Lawal, D.U. Removal of heavy metal ions from wastewater: A comprehensive and critical review. *npj Clean Water* **2021**, *4*, 36. [CrossRef]
2. Lin, G.; Zeng, B.; Li, J.; Wang, Z.; Wang, S.; Hu, T.; Zhang, L. A systematic review of metal organic frameworks materials for heavy metal removal: Synthesis, applications and mechanism. *Chem. Eng. J.* **2023**, *460*, 141710.
3. Dhokpande, S.R.; Deshmukh, S.M.; Khandekar, A.; Sankhe, A. A review outlook on methods for removal of heavy metal ions from wastewater. *Sep. Purif. Technol.* **2024**, *350*, 127868.
4. Zamora-Ledezma, C.; Negrete-Bolagay, D.; Figueroa, F.; Zamora-Ledezma, E.; Ni, M.; Alexis, F.; Guerrero, V.H. Heavy metal water pollution: A fresh look about hazards, novel and conventional remediation methods. *Environ. Technol. Innov.* **2021**, *22*, 101504.

5. Wang, S.; Song, W.; Liu, E.; Zhao, P.; Ng, H.Y.; Wang, X. Efficient, facile and recyclable coating strategy to improve heavy metals removal by UF membrane in drinking water purification. *Sep. Purif. Technol.* **2025**, *363*, 131995.
6. Satyam, S.; Patra, S. Innovations and challenges in adsorption-based wastewater remediation: A comprehensive review. *Heliyon* **2024**, *10*, e29573. [PubMed]
7. Pellenz, L.; de Oliveira, C.R.S.; Júnior, A.H.d.S.; da Silva, L.J.S.; de Souza, A.A.U.; Souza, S.M.d.A.G.U.d.; Borba, F.H.; da Silva, A. A comprehensive guide for characterization of adsorbent materials. *Sep. Purif. Technol.* **2023**, *305*, 122435.
8. Singh, S.; Kapoor, D.; Khasnabis, S.; Singh, J.; Ramamurthy, P.C. Mechanism and kinetics of adsorption and removal of heavy metals from wastewater using nanomaterials. *Environ. Chem. Lett.* **2021**, *19*, 2351–2381.
9. Liu, P.; Yan, T.; Zhang, J.; Shi, L.; Zhang, D. Separation and recovery of heavy metal ions and salt ions from wastewater by 3D graphene-based asymmetric electrodes: Via capacitive deionization. *J. Mater. Chem. A* **2017**, *5*, 14748–14757.
10. Björklund, K.; Li, L.Y. Adsorption of organic stormwater pollutants onto activated carbon from sewage sludge. *J. Environ. Manag.* **2017**, *197*, 490–497. [CrossRef]
11. Largitte, L.; Pasquier, R. A review of the kinetics adsorption models and their application to the adsorption of lead by an activated carbon. *Chem. Eng. Res. Des.* **2016**, *109*, 495–504. [CrossRef]
12. Gupta, K.; Joshi, P.; Gusain, R.; Khatri, O.P. Recent advances in adsorptive removal of heavy metal and metalloid ions by metal oxide-based nanomaterials. *Coord. Chem. Rev.* **2021**, *445*, 214100. [CrossRef]
13. Yang, C.; Niu, D.; Zhang, F.; Zhong, Y.; Cao, T.; Li, L.; Liu, Y. Absorption mechanisms of lead in aqueous solutions with hydrous manganese dioxide. *Water Sci. Technol.* **2018**, *77*, 2454–2462. [CrossRef] [PubMed]
14. Ravindranath, R.; Roy, P.; Periasamy, A.P.; Chen, Y.W.; Liang, C.T.; Chang, H.T. Fe_2O_3/Al_2O_3 microboxes for efficient removal of heavy metal ions. *New J. Chem.* **2017**, *41*, 7751–7757. [CrossRef]
15. Rajput, A.; Sharma, P.P.; Yadav, V.; Gupta, H.; Kulshrestha, V. Synthesis and characterization of different metal oxide and GO composites for removal of toxic metal ions. *Sep. Sci. Technol.* **2019**, *54*, 426–433. [CrossRef]
16. Farhan, A.; Khalid, A.; Maqsood, N.; Iftekhar, S.; Sharif, H.M.A.; Qi, F.; Sillanpää, M.; Asif, M.B. Progress in layered double hydroxides (LDHs): Synthesis and application in adsorption, catalysis and photoreduction. *Sci. Total Environ.* **2024**, *912*, 169160. [CrossRef] [PubMed]
17. Ahmed, M.A.; Mohamed, A.A. A systematic review of layered double hydroxide-based materials for environmental remediation of heavy metals and dye pollutants. *Inorg. Chem. Commun.* **2023**, *148*, 110325. [CrossRef]
18. Alnasrawi, F.A.; Mohammed, A.A. Mohammed, Enhancement of Cd^{2+} removal on CuMgAl-layered double hydroxide/montmorillonite nanocomposite: Kinetic, isotherm, and thermodynamic studies. *Arab. J. Chem.* **2023**, *16*, 104471. [CrossRef]
19. Qi, Y.; Wei, L.; Shi, D.; Cai, W.; Guo, L. Al-Li Alloy Chemical Milling Waste Solution Synthesis of γ-AlOOH Bundles for Cr(VI) Rapid Adsorption. *ChemistrySelect* **2020**, *5*, 5732–5741. [CrossRef]
20. Vo, T.K.; Park, H.-K.; Nam, C.-W.; Kim, S.-D.; Kim, J. Facile synthesis and characterization of γ-AlOOH/PVA composite granules for Cr(VI) adsorption. *J. Ind. Eng. Chem.* **2018**, *60*, 485–492. [CrossRef]
21. Zhang, Y.X.; Jia, Y.; Jin, Z.; Yu, X.Y.; Xu, W.H.; Luo, T.; Zhu, B.J.; Liu, J.H.; Huang, X.J. Self-assembled, monodispersed, flower-like γ-AlOOH hierarchical superstructures for efficient and fast removal of heavy metal ions from water. *CrystEngComm* **2012**, *14*, 3005. [CrossRef]
22. Granados-Correa, F.; Corral-Capulin, N.G.; Olguín, M.T.; Acosta-León, C.E. Comparison of the Cd(II) adsorption processes between boehmite (-AlOOH) and goethite (-FeOOH). *Chem. Eng. J.* **2011**, *171*, 1027–1034. [CrossRef]
23. Zheng, L.; Gao, Y.; Du, J.; Zhang, W.; Huang, Y.; Zhao, Q.; Duan, L.; Liu, Y.; Naidu, R.; Pan, X. Single and Binary Adsorption Behaviour and Mechanisms of Cd^{2+}, Cu^{2+} and Ni^{2+} onto Modified Biochar in Aqueous Solutions. *Processes* **2021**, *9*, 1829. [CrossRef]
24. Zhang, Z.; He, S.; Zhang, Y.; Zhang, K.; Wang, J.; Jing, R.; Yang, X.; Hu, Z.; Lin, X.; Li, Y. Spectroscopic investigation of Cu^{2+}, Pb^{2+} and Cd^{2+} adsorption behaviors by chitosan-coated argillaceous limestone: Competition and mechanisms. *Environ. Pollut.* **2019**, *254*, 112938. [CrossRef] [PubMed]
25. Lu, X.; Wang, F.; Li, X.Y.; Shih, K.; Zeng, E.Y. Adsorption and Thermal Stabilization of Pb^{2+} and Cu^{2+} by Zeolite. *Ind. Eng. Chem. Res.* **2016**, *55*, 8767–8773. [CrossRef]
26. Tan, P.; Sun, J.; Hu, Y.; Fang, Z.; Bi, Q.; Chen, Y.; Cheng, J. Adsorption of Cu^{2+}, Cd^{2+} and Ni^{2+} from aqueous single metal solutions on graphene oxide membranes. *J. Hazard. Mater.* **2015**, *297*, 251–260.

Disclaimer/Publisher's Note: The statements, opinions and data contained in all publications are solely those of the individual author(s) and contributor(s) and not of MDPI and/or the editor(s). MDPI and/or the editor(s) disclaim responsibility for any injury to people or property resulting from any ideas, methods, instructions or products referred to in the content.